Sensors and Materials, Vol. 38, No. 8 (2026) 4343–4356
MYU Tokyo

S & M 4569

Laser Spot Periodic Heating Radiation Thermometry for Measuring Thermal Diffusivity of Anisotropic Materials

Seiichiro Sando,[1,2*] Hiromichi Ohta,[1] and Tsuyoshi Nishi[1]

[1]Ibaraki University, Hitachi Campus 4-12-1 Nakanarusawa-cho, Hitachi-shi, Ibaraki 316-8511, Japan
[2]BETHEL Co., Ltd.,
4-3-18, Tsuchiura Brick Bldg. 1F, Sakura-machi, Tsuchiura-shi, Ibaraki 300-0037, Japan

(Received March 27, 2026; Accepted May 14, 2026)

Keywords: laser spot periodic heating radiation thermometry, thermal diffusivity, thermal conductivity, anisotropy, graphite sheets, finite element method

The accurate evaluation of in-plane and out-of-plane thermal diffusivities is crucial for thermally anisotropic materials. In this study, we propose a measurement and analysis framework based on laser spot periodic heating radiation thermometry for such materials. For in-plane thermal diffusivity, the conventional method based on the distance dependence of the phase lag was applied, while ensuring that the combined choice of modulation frequency and measurement distance range satisfied both the required number of thermal waves and the validity of the 1D heat-diffusion approximation. For out-of-plane thermal diffusivity, a finite element method was employed to reproduce effects that cannot be neglected under out-of-plane measurement conditions, including the finite spatial distributions of laser heating and thermal detection, as well as thermal-wave reflection at material surfaces. The validity of the proposed approach was first confirmed using a pure copper sample and well-established literature values, demonstrating that the appropriate wave-number selection and accurate reproduction of the measurement configuration lead to reliable thermal diffusivity evaluation. The methodology was then applied to graphite sheets as a demonstration case, and physically reasonable consistency with existing data was obtained. These results indicate that the proposed framework provides a practical and reliable method for evaluating anisotropic thermal diffusivity.

1. Introduction

Laser spot periodic heating radiation thermometry enables the evaluation of in-plane and out-of-plane thermal diffusivities by detecting the phase lag of the temperature response at the rear surface using a noncontact infrared radiation thermometer.[1,2] This method originates from the fundamental concepts of AC calorimetry and shares the common principle of evaluating thermal diffusivity through the phase response under periodic heating. While AC calorimetry measures the rear-surface temperature using a contact sensor such as a thermocouple,[3,4] laser spot periodic heating radiation thermometry relies on a noncontact infrared thermometer for

*Corresponding author: e-mail: s-sandoh@btl-hrd.jp
https://doi.org/10.18494/SAM6318

ISSN 0914-4935 © MYU K.K.
https://myukk.org/

detection. In AC calorimetry, the ability to adjust the heating frequency allows the method to accommodate various measurement conditions and sample geometries, enabling its application to a wide range of materials, including isotropic metals, heterogeneous materials, and anisotropic materials.(4) These advantages also extend to laser spot periodic heating radiation thermometry, given its reliance on phase-based analysis under periodic heating.

In thermal diffusivity analysis, analytical solutions can be fitted to experimentally obtained phase lag data to simultaneously determine the in-plane and out-of-plane thermal diffusivities in both AC calorimetry and laser spot periodic heating radiation thermometry.(4–7) Additionally, the in-plane thermal diffusivity can also be determined from the distance dependence of the phase lag between the heating and detection points.(1–3) In both approaches, the in-plane thermal diffusivity can be evaluated accurately. In contrast, the out-of-plane thermal diffusivity obtained through model-based fitting often exhibits non-negligible errors, which have been estimated to range from 11 to 52% in graphite sheet (GS) measurements.(5) This discrepancy arises because the fitting procedure commonly employs an idealized point-source model, although the actual laser heating intensity has a finite spatial extent. However, previous studies have not sufficiently accounted for this finite spatial extent in out-of-plane thermal diffusivity analysis.

Therefore, in this study, Gaussian-shaped heating and detection profiles(8) are explicitly incorporated into the analysis of out-of-plane thermal diffusivity. Additionally, the conventional in-plane analysis based on the distance dependence of the phase lag is refined by clarifying the conditions under which the one-dimensional approximation remains valid. For the measurement of out-of-plane thermal diffusivity, the finite element method (FEM) is employed because it enables the straightforward implementation of Gaussian heating and detection profiles while accurately modeling the specimen geometry,(9) including edge reflections,(7,10) thereby allowing thermal diffusivity to be determined through comparison with experimental data. The in-plane thermal diffusivity is evaluated from the distance dependence of the phase lag using an analytical framework based on 1D in-plane thermal-wave propagation. To ensure the validity of this framework, measurements are performed under conditions in which the effects of the finite heating and detection regions, as well as out-of-plane heat transfer, are negligible. A GS is selected as the target material because it exhibits strong thermal anisotropy, characterized by high in-plane and low out-of-plane thermal diffusivities,(5,6) making it well suited for evaluating improvements in analytical accuracy. Furthermore, GSs exhibit flexibility, low density, and high thermal conductivity, which have led to their widespread industrial application and an increasing demand for the accurate characterization of their thermal properties.

2. Experimental and Analytical Methods

2.1 Measurement principle

Considering a point heat source with the power $P_0 e^{i2\pi ft}$ applied to a thin sample with the thermal diffusivity D at a frequency f, the temperature response T_{AC} at time t and at a distance r from the heat source point is given by(7)

$$T_{AC} = \frac{P_0}{4\pi Drc} \cdot e^{-kr+i(2\pi ft-kr)}, \tag{1}$$

where c is the specific heat and k is the wave number of the temperature wave expressed as

$$k = \sqrt{\frac{\pi f}{D}}. \tag{2}$$

At point r, the phase lag θ against the heat source is defined as

$$\theta = -kr. \tag{3}$$

Thus, the thermal diffusivity can be determined from the relationship between the phase lag and the propagation distance.

2.2 Measurement equipment

Figure 1 shows a schematic diagram of the experimental apparatus, the Thermowave Analyzer TA (BETHEL Co., Ltd., Ibaraki, Japan).[11] The overall configuration of the apparatus has been described in detail by the manufacturer,[11] and only a brief outline is given here. A laser beam, modulated at a frequency controlled by a function generator, is focused onto the sample surface. The modulated laser irradiation generates a thermal wave at the surface, which propagates through the sample and is detected at the opposite surface by radiation thermometry.

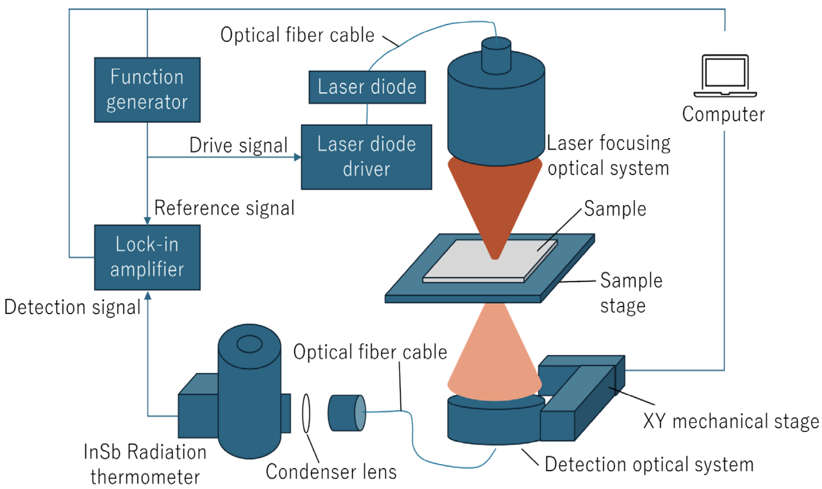

Fig. 1. (Color online) Experimental setup used in this study.

The phase lag of the detected modulated signal relative to the reference signal from the function generator is analyzed using a lock-in amplifier. For the in-plane thermal diffusivity measurements, a mechanical stage is employed to translate the detection position. The apparatus used in this study features a laser beam with a full width at half maximum (FWHM) of 125 μm and a detection area with an FWHM of 885 μm.

2.3 Analytical procedures

To determine the measurement conditions for the periodic heating method, an appropriate number of waves must be selected. The number of waves is defined as the ratio of the wavelength to the propagation distance, where the wavelength is determined by the frequency and material properties. A suitable range for the number of waves is ~1–2. When the number of waves is limited, the resulting small phase lag renders the evaluated thermal diffusivity highly sensitive to even minor phase detection errors. Conversely, when the number of waves is sufficiently large to cause a substantial attenuation of the temperature response, the accuracy of phase analysis during lock-in detection deteriorates.

2.3.1 Analysis of in-plane thermal diffusivity

For the analysis of the in-plane thermal diffusivity, the conventional approach based on the distance dependence of the phase lag was employed. To ensure analytical validity, it is essential to select an appropriate distance range in which the assumption of 1D heat diffusion is valid.(4) In addition, a sufficient number of waves must be ensured. Notably, the wave-number condition alone is a necessary but not sufficient for reliable analysis and must be considered together with the validity of the 1D approximation. In the vicinity of the heating-region center, the phase lag exhibits nonlinear behavior with respect to distance owing to the effect of out-of-plane heat transport and the finite sizes of the heating and detection regions. From a geometrical standpoint, the 1D approximation becomes increasingly valid as the in-plane propagation distance becomes sufficiently larger than the sample thickness, such that the actual heat propagation pathway is accurately approximated by its in-plane projection. Under this condition, and when the in-plane thermal diffusion length is appropriately selected relative to the sample thickness and the sizes of the heating and detection regions, the temperature field is predominantly governed by in-plane heat transport. As a result, the phase lag exhibits a linear dependence on the distance. Therefore, the distance and frequency ranges were selected such that the analytical result remained within the linear region. According to Eqs. (2) and (3), when 1D heat diffusion is assumed, the in-plane thermal diffusivity can be determined from the slope of the phase lag with respect to distance, as expressed in

$$\frac{\partial \theta}{\partial r} = -\sqrt{\frac{\pi f}{D_{||}}}, \tag{4}$$

where $D_{||}$ denotes the thermal diffusivity in the in-plane direction.

2.3.2 Analysis of out-of-plane thermal diffusivity

To perform the out-of-plane measurements, the thermal diffusivity was analyzed using a fully 3D FEM model, in which in-plane heat diffusion was explicitly considered. The in-plane thermal diffusivity used in the model was independently determined in advance under conditions where the 1D in-plane approximation was valid. This FEM approach, implemented in COMSOL Multiphysics software (COMSOL Inc., Burlington, MA, USA), enables the accurate reproduction of the measurement configuration and the appropriate treatment of the effects that cannot be neglected, including the finite widths of the laser heating and detector sensitivity distributions as well as the thermal-wave reflections at the sample surfaces. In the finite element analysis, a periodic heat input with a Gaussian spatial distribution having an FWHM of 125 μm was applied to the heating surface to simulate laser irradiation. Adiabatic boundary conditions were imposed on all outer surfaces. Thermal anisotropy was introduced by assigning independent in-plane and out-of-plane thermal conductivities. The temperature distribution on the rear surface was calculated, and the detected temperature was obtained by convolving it with a Gaussian detection sensitivity function having an FWHM of 885 μm. The resulting temporal temperature response was then analyzed by sinusoidal fitting using Mathematica (Wolfram Research, Champaign, IL, USA), from which the phase lag was determined. The fitting function is given by[12]

$$T(t, A, \theta, a, b, c) = A\sin(2\pi ft - \theta) + at^2 + bt + c, \tag{5}$$

where T is the rear-surface temperature response; A is the amplitude; and a, b and c are the baseline coefficients that account for the gradual temperature increase due to the cumulative heat input. The out-of-plane thermal diffusivity was determined by identifying the value that yielded the closest agreement between the FEM-calculated and experimentally measured values, with phase lag at each measurement position. The evaluation was performed in the vicinity of the heating-surface center to minimize the effect of in-plane heat diffusion. The excitation frequency was selected such that the number of waves across the out-of-plane direction was within an appropriate range, ensuring accurate measurement. In the FEM model, a 3D mesh was generated by sweeping the in-plane mesh geometry along the out-of-plane direction and subdividing it into layered elements, allowing the consistent control of the element size in both the in-plane and out-of-plane directions. A 3D coordinate system was employed in the finite element model to ensure the general applicability of the proposed analytical framework. This choice is expected to facilitate the future development of materials with 3D heterogeneous microstructures, including dispersion-type composites. For the determination of the phase lag of the FEM-calculated response and the elimination of the effect of transient behavior, the response during the initial 17 periods was discarded, and fitting was performed using the data from the 18th to 20th periods, where a steady periodic state was confirmed.

2.4 Samples

To verify the reliability of the experimental apparatus and analytical procedure, additional measurements were performed using a pure copper specimen (50 × 50 mm^2, 507 μm thickness).

The thermal diffusivity was calculated to be 118 × 10^{-6} m^2/s on the basis of the reported thermal conductivity,(13,14) the specific heat of copper at room temperature [(379 J/kg/K),(12) equivalent to 24.44 J/mol/K(15)], and the density.(13)

Table 1 shows the properties of the GS samples (RS Components, Ltd., Kanagawa, Japan) used in the current study. These properties are shown for illustrative purposes only; they were not treated as absolute or reference values and should not be interpreted as benchmarks for validating the proposed method. Instead, they allow a comparison with the results obtained via two different approaches, namely, the catalog values for in-plane conductivity and the independently measured values obtained using the frequency-dependent method described in the literature(2) for out-of-plane conductivity. Such a comparison demonstrates that the proposed method produces physically reasonable measurements, without implying that the GS data themselves are exact. The thickness, specific heat, and density of each sample were measured using a micrometer (MDC-25MXT, Mitutoyo Corporation, Kanagawa, Japan), a differential scanning calorimeter (DSC200, Hitachi High-Tech Corporation, Tokyo, Japan), and an electronic balance (HR-202i, A&D Company, Ltd., Tokyo, Japan), respectively.

3. Results

3.1 Uncertainty of thermal diffusivity analysis

Since the thermal properties of pure copper are well established in the literature,(12–14) it serves as a suitable benchmark material for validating the present measurement and analysis procedure. Measurements were therefore performed on pure copper to confirm the appropriateness of the wave-number selection, the treatment of finite heating and detection sizes, and the thermal-wave reflection effects.

3.1.1 Uncertainty of in-plane thermal diffusivity analysis

Figure 2 shows the phase lag as a function of the distance between the centers of the heating and detection regions, as obtained from the measurement of a pure copper sample at 5 Hz. This figure clearly indicates that the relationship between the phase lag and the distance approaches linearity as the distance increases. The thermal diffusivity of pure copper was calculated to be

Table 1
GS sample properties.

Sample	Thickness (μm)	Thermal conductivity (W/m·K)		Specific heat (J/kg·K)	Density (kg/m^3)	Thermal diffusivity (×$10^{-6}$$m^2$/s)		Size (mm)
		In-plane	Out-of-plane			In-plane	Out-of-plane	
GS844	844	350	5.08	660	1080	491	7.13	50 × 50
GS522	522		4.12		1380	384	4.52	

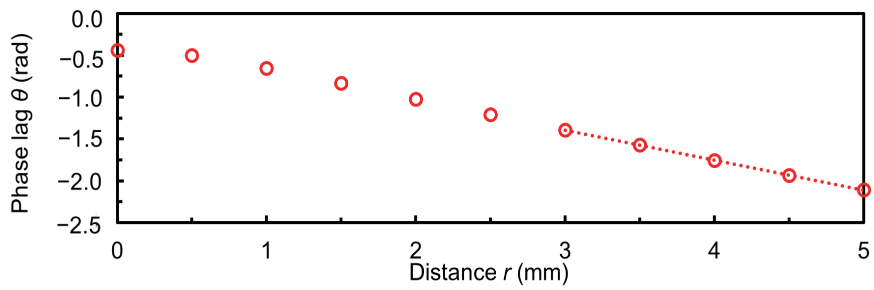

Fig. 2. (Color online) Distance dependence of the phase lag obtained from the measurement of pure copper at 5 Hz.

122 × 10^{-6} m^2/s at 5 Hz, with a slope of −0.3586 being obtained in the range of 3–5 mm. The corresponding number of waves in this range was estimated to be between 1.1 and 1.8.

Table 2 shows the in-plane thermal diffusivities obtained at modulation frequencies of 1, 5, 20, 36, and 145 Hz. The results obtained at 1, 5, and 20 Hz were within ±10% of the literature value for pure copper, whereas those obtained at 36 and 145 Hz showed larger deviations. At 36 and 145 Hz, although the number of waves was sufficient, the condition could not be satisfied within the distance range where heat diffusion can be regarded as 1D, thereby reducing the reliability of the in-plane phase analysis. In contrast, at 1, 5, and 20 Hz, it was possible to adjust the number of waves to an appropriate range by selecting suitable measurement distances, under which both the phase lag and the temperature-response amplitude were sufficiently maintained, resulting in higher evaluation accuracy. These results demonstrate that the number of waves is an effective dimensionless parameter for organizing and optimizing the evaluation accuracy of in-plane thermal diffusivity, particularly in identifying measurement conditions under which the 1D in-plane heat propagation approximation is valid.

3.1.2 Uncertainty of out-of-plane thermal diffusivity analysis

Figure 3 shows the FEM model constructed using the actual specimen dimensions and the generated mesh. The mesh design was determined from the spatial characteristics of the Gaussian heating profile and the thermal diffusion length. In the vicinity of the laser heating center, where the temperature gradient was most pronounced, a sufficiently fine mesh was employed, with the element size set to be smaller than the FWHM of the heating distribution. As the distance from the heating center increased, the mesh size gradually increased while maintaining sufficient resolution relative to the thermal diffusion length corresponding to the modulation frequency. Using this strategy, a swept 3D mesh consisting of ~11000 elements was constructed. The in-plane mesh size was determined to be <100 μm in the central region and ~500 μm in the outer region, while the out-of-plane mesh size was ~500 μm. Owing to the automatic mesh growth scheme, intermediate regions locally exhibited relatively larger element sizes; however, a sufficiently fine resolution was maintained in the region of interest. This mesh design enabled an accurate representation of the steep temperature gradient in the heating

Table 2
Results obtained during the measurement of pure copper.

Frequency (Hz)	Reference	1	5	20	36	145
Distance range (mm)	—	6.0–7.0	3.0–5.0	1.5–2.5	1.0–2.0	0.5–1.0
Number of waves	—	1.0–1.1	1.1–1.8	1.1–1.8	1.0–2.0	1.0–2.0
Thermal diffusivity ($\times 10^{-6}$m^2/s)	118	127	122	125	145	427

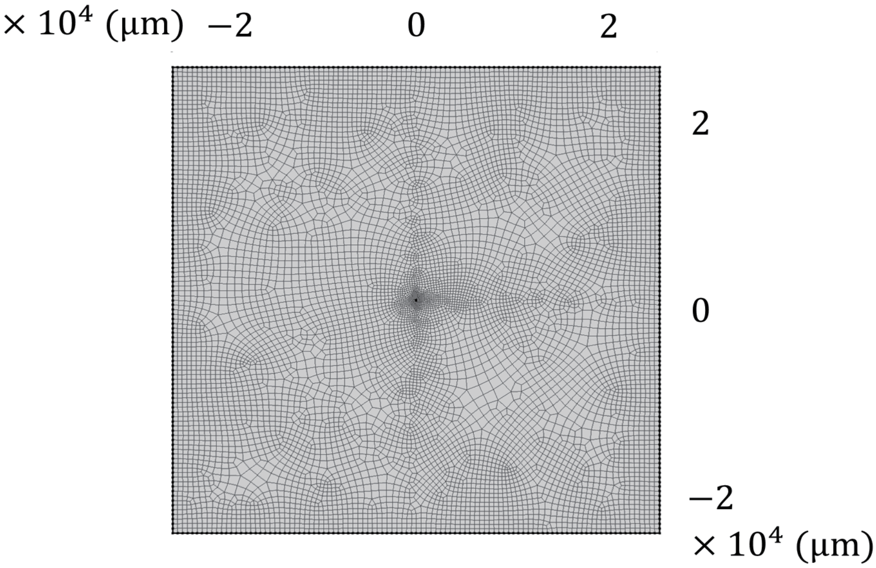

Fig. 3. In-plane element mesh of the copper model at 580 Hz.

region while maintaining reasonable computational efficiency in the outer region. Although the FEM model is not strictly axisymmetric owing to the unstructured mesh, the mesh resolution in the vicinity of the heating and detection regions was sufficiently fine to ensure that any azimuthal variation in the calculated phase lag remained negligible within the practical evaluation accuracy of the present study. Accordingly, the phase lag was treated as a function of the radial distance from the heating center.

To verify the validity of the FEM analysis, Fig. 4 shows the distance dependence of the phase lag between the centers of the heating and detection regions for a pure copper sample at 580 Hz. The figure also compares the experimental results with the theoretical solution obtained from the isotropic analytical model[8] using the physical properties of pure copper, the 1D model described by Eq. (3), and the FEM results. The modulation frequency of 580 Hz was selected such that the corresponding out-of-plane wave number was ~2, which lies within the appropriate range for reliable evaluation. The analytical model was formulated for a plate that is effectively unbounded in the in-plane direction and finite in the out-of-plane direction, with adiabatic boundary conditions applied to both surfaces and laser energy assumed to be absorbed at the surface. The theoretical temperature field was integrated with the detector sensitivity distribution to obtain the observable temperature response, from which the phase lag was evaluated. Although both the actual specimen and the finite element model exhibit finite in-plane dimensions, the distance from the heating position to the specimen edge and the measurement

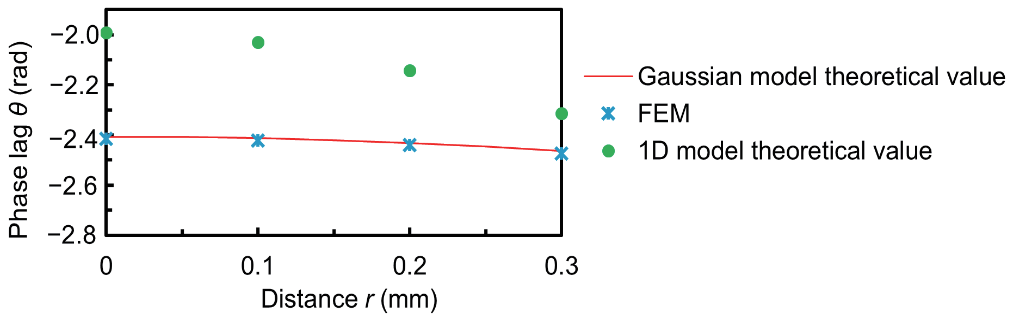

Fig. 4. (Color online) Distance dependence of the phase lag calculated by FEM and using the analytical model for copper at 580 Hz.

frequency satisfy conditions that prevent thermal waves at the specimen edge from affecting the measurement region.(3) Under these conditions, the finite specimen can be regarded as semi-infinite in the in-plane direction. The analysis was restricted to the region near the center of the heating area, where heat transport in the out-of-plane direction predominantly affected the distance dependence of the phase lag. Additionally, the modulation frequency was selected such that the number of thermal waves in the out-of-plane direction was within an appropriate range, ensuring that both the phase lag and the temperature-response amplitude were sufficiently maintained. The FEM-calculated phase lag behavior corresponded well with the analytical solution for a semi-infinite plate with periodic surface heating, derived under the same theoretical framework and boundary conditions as those reported in the literature,(8) confirming the validity of the FEM analysis. A comparison with the 1D model further revealed that the 1D approximation fails to reproduce the observed distance dependence of the phase lag under the present experimental conditions.

Figure 5 illustrates the distance-dependent phase lag between the centers of the heating and detection regions for a pure copper sample at 580 Hz. This plot includes the experimental results, FEM results, and FEM results obtained by varying the out-of-plane thermal diffusivity by ±10% from the reference value. This ±10% variation was introduced to visualize the sensitivity of the phase lag to the out-of-plane thermal diffusivity. Within this range, the FEM-calculated phase lag exhibited an approximately linear dependence on the out-of-plane thermal diffusivity. The comparison of the FEM results obtained with ±10% variation shows that the experimental data lie well within this range. Owing to this near-linear relationship, the relative deviation of the experimental phase lag from the reference FEM result can be directly translated into a corresponding uncertainty in the out-of-plane thermal diffusivity. Considering that the observed phase-lag deviation is substantially smaller than the change induced by a ±10% variation, the effective uncertainty in the evaluated out-of-plane thermal diffusivity is estimated to be approximately ±3%. These findings demonstrate that the out-of-plane thermal diffusivity can be reliably determined. This result also confirms the validity of excitation-frequency selection based on the out-of-plane wave number, as well as the FEM-based treatment of finite heating and detection sizes and the thermal-wave reflection effects.

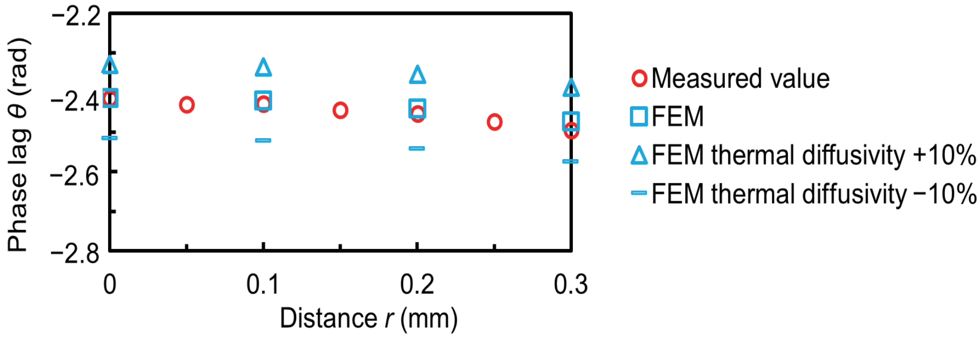

Fig. 5. (Color online) Distance dependence of the phase lag calculated by FEM and measured value for copper at 580 Hz.

3.2 Result of GS thermal diffusivity analysis

The experimental conditions for the GS samples were determined by directly applying the wave-number selection criteria and FEM-based treatment validated through benchmark measurements on pure copper. The treatment accounted for heating, detection, and thermal-wave reflection effects. Figure 6 shows the slope derived from the distance dependence of the phase lag in GS522 at 5 Hz, evaluated over a measurement distance range of 5.0–7.0 mm, corresponding to a wave-number range of 1.1–1.5. Using Eq. (4), we calculated the in-plane thermal diffusivity of GS522 from a slope of −0.2050 as 374 × 10^{-6} m^2/s. Figure 7 shows a comparison of the experimental results with the FEM calculations, in which the out-of-plane thermal diffusivity was treated as a fitting parameter at 20 Hz, corresponding to an out-of-plane wave number of 2.0. The FEM employed the meshing strategy described in Sect. 2.3.2, with an in-plane mesh size of ~100 µm in the central region that gradually increased to ~2000 µm toward the outer boundaries and an out-of-plane mesh size of ~100 µm. The final mesh consisted of ~55000 elements and nodes. The same measurement procedure and meshing strategy, with comparable element-size distributions, were applied to GS844. Table 3 shows the experimental conditions and thermal diffusivities obtained for the GS samples of different thicknesses.

4. Discussion

In periodic heating measurements, the accuracy of the evaluated thermal diffusivity critically depends on the appropriate design of the measurement conditions. For in-plane measurements, this requires the simultaneous satisfaction of two conditions: the appropriate selection of the wave number and the identification of a distance range in which the 1D heat-diffusion approximation is valid. For out-of-plane measurements, in addition to wave-number selection, it is essential to correctly account for finite heating and detection areas, as well as the thermal-wave reflection effects at the sample surface. The importance of these conditions was demonstrated through measurements on pure copper, whose thermal diffusivity is well established. When the measurement conditions were designed to satisfy the above requirements, the present method yielded thermal diffusivities in good agreement with literature values.

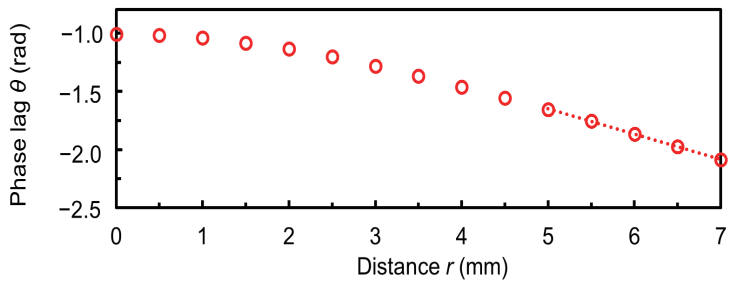

Fig. 6. (Color online) Distance dependence of the phase lag calculated by measurement of the GS522 specimen at 5 Hz.

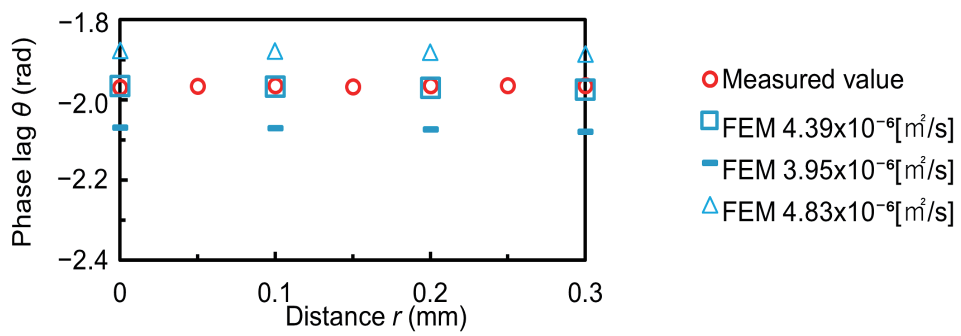

Fig. 7. (Color online) Distance dependence of the phase lag calculated by FEM and measurement of the GS522 specimen at 20 Hz.

Table 3
Conditions employed for measurement of GSs and corresponding results.

Sample	Frequency in-plane (Hz)	Distance for analysis (mm) (Number of waves)	Frequency out-of-plane (Hz) (Number of waves)	Thermal diffusivity ($\times 10^{-6}$m^2/s) (relative error from benchmark)		Thermal conductivity (W/m·K)	
				In-plane	Out-of-plane	In-plane	Out-of-plane
GS844	2	6.6–7.5 (0.8–0.9)	10 (1.8)	436 (−11.2%)	7.15 (+3.9%)	312	5.1
GS522	5	5.0–7.0 (1.1–1.5)	20 (2.0)	333 (−13.2%)	4.39 (−2.9%)	303	4.0

Previous studies reported errors of 11–52% in the evaluation of the cross-plane thermal diffusivity of GSs.[5] In contrast, the present method reduced this error to less than approximately 4% for the GSs examined in this study, demonstrating a significant improvement in accuracy. This result confirms that the proposed measurement and analysis framework provides reliable evaluations when the underlying physical assumptions are appropriately satisfied. On the basis of this validation, the same principles for measurement condition design and analysis were applied to anisotropic GS materials. Although absolute reference values are not available for the thermal diffusivity of GSs, the existing data obtained using different experimental approaches provide practical benchmarks for assessing consistency. The thermal diffusivities obtained in the present study were comparable in magnitude to the reported values for both in-plane and out-of-plane directions, indicating that the essential features of thermal transport in GS materials were appropriately captured. Although some discrepancies remain between the present results and previously reported values, they are relatively small and can reasonably be attributed to differences in measurement principles, analysis assumptions, and sample characteristics. Overall, the consistency observed under carefully controlled measurement conditions suggests that the present methodology offers a physically sound and useful approach for evaluating anisotropic thermal diffusivities. The applicable range of the present method is primarily governed by the wave number, which depends on both the thermal diffusivity and the modulation frequency. By appropriately selecting the modulation frequency, heating-to-detection distance, and specimen thickness, the required measurement conditions can be established over wide ranges of thermal diffusivities and anisotropy ratios. Therefore, the present method is expected to be broadly applicable to anisotropic materials, provided that the measurement conditions satisfy the assumptions underlying the in-plane and out-of-plane analyses.

5. Conclusions

In this study, laser spot periodic heating radiation thermometry was applied to evaluate the in-plane and out-of-plane thermal diffusivities of anisotropic GSs. The validity of the measurement and analysis procedure was first verified using copper, for which reliable reference data are available. On the basis of this validated framework, the same experimental and analytical approach was applied to GS exhibiting strong thermal anisotropy. The obtained results showed good consistency with existing data, indicating that the present methodology provides a physically reasonable and reliable approach for evaluating thermal diffusivity in anisotropic materials. The present method is also applicable to materials exhibiting in-plane anisotropy by incorporating the directional thermal diffusivities into the 3D FEM analysis. However, in such cases, the principal axes of thermal anisotropy must be identified in advance and the measurement geometry should be appropriately aligned.

Acknowledgments

The authors are deeply grateful to Kimihito Hatori, Tetsuya Otsuki, Takaaki Awano, Hidenori Noguchi, Chikako Kobayashi, Hitomi Nagamine, Nana Koyama, and Junichi Suzuki of BETHEL Co., Ltd. (Ibaraki, Japan).

References

1 K. Hatori, T. Awano, T. Otsuki, K. Uetani, and H. Nagano: Int. J. Thermophys. **43** (2022) 84. https://doi.org/10.1007/s10765-022-03009-w
2 T. Ishizaki and H. Nagano: Int. J. Thermophys. **36** (2015) 2577. https://doi.org/10.1007/s10765-014-1755-5

3 M. Kuribara and H. Nagano: J. Electron. Cool. Thermal Control **5** (2015) 15. https://doi.org/10.4236/jectc.2015.51002
4 Y. Zhang, R. Xu, Y. Liu, Q. Jiang, Q. Li, Y. Liu, and J. Wang: Int. J. Heat Mass Trans. **227** (2024) 125536. https://doi.org/10.1016/j.ijheatmasstransfer.2024.125536.
5 H. Nagano, H. Kato, A. Ohnishi, and Y. Nagasaka: Int. J. Thermophys. **22** (2001) 301. https://doi.org/10.1023/A:1006780208048
6 H. Nagano, A. Ohnishi, and Y. Nagasaka: J. Thermophys. Heat Trans. **15** (2001) 347. https://doi.org/10.2514/2.6614
7 H. Kato, T. Baba, and M. Okaji: Meas. Sci. Technol. **12** (2001) 2074. https://doi.org/10.1088/0957-0233/12/12/307
8 S. Nagata, T. Nishi, S. Miyake, N. Azuma, K. Hatori, T. Awano, and H. Ohta: Materials **13** (2020) 4848. https://doi.org/10.3390/ma13214848
9 N. Stojanovic, J. Yun, E. B. K. Washington, J. M. Berg, M. W. Holtz, and H. Temkin: J. Microelectromech. Syst. **16** (2007) 1269. https://doi.org/10.1109/JMEMS.2007.900877
10 I. Hatta, R. Kato, and A. Maesono: Jpn. J. Appl. Phys. **26** (1987) 475. https://doi.org/10.1143/JJAP.26.475
11 Thermowave Analyzer Measuring Principle and Equipment: (Application Sheet TA-001E) (2022) https://hrd-thermal.jp/en/apparatus/application_sheet/TA/TA001E_TA_theory_equipment_220803_r01.pdf (accessed January 2026).
12 S. Sando, T. Otsuki, H. Ohta, T. Nishi, and K. Hosono: JSME Proc. ROMBUNNO.J224-01 (2023). https://doi.org/10.1299/jsmemecj.2023.J224-01 (in Japanese).
13 Japan Society of Thermophysical Properties (Ed.), Shinpen Thermophysical Properties Handbook (Yokendo, Tokyo (2008) pp. 20 (in Japanese).
14 C. Y. Ho, R. W. Powell, and P. E. Liley: J. Phys. Chem. Ref. Data **1** (1972) 279. https://doi.org/10.1063/1.3253100
15 B. J. McBride, S. Gordon, and M. N. Reno: "Thermodynamic Data for Fifty Reference Elements", Report No. ADA275283, Defense Technical Information Center (DTIC), U.S. Department of Defense (1993). https://apps.dtic.mil/sti/html/tr/ADA275283/index.html (accessed January 2026).

About the Authors

Seiichiro Sando received his B.S. degree from Tohoku University, Japan, in 2020. Since 2021, he has been a research engineer at BETHEL Co., Ltd. In 2024, he enrolled in the doctoral program at Ibaraki University. His research interests include the development of steady-state methods and laser spot periodic heating radiation thermometry. (s-sandoh@btl-hrd.jp)

Hiromichi Ohta received his B.S., M.S., and Ph.D. degrees from Tohoku University, Japan, in 1978, 1980, and 1984, respectively. From 1984 to 2008, he served as a research associate and associate professor at Ibaraki University, Japan. Since 2008, he has been a professor at Ibaraki University. His research interests include thermophysical properties, computational material science, composite materials, and silicate melts. (hiromichi.ohta.ys@vc.ibaraki.ac.jp)

Tsuyoshi Nishi received his B.S. degree from Tokyo University of Science, Japan, in 1999 and his M.S. and Ph.D. degrees from Tohoku University, Japan, in 2001 and 2004, respectively. From 2004 to 2021, he was a research scientist at the Japan Atomic Energy Agency and an associate professor at Ibaraki University, Japan. Since 2021, he has been a professor at Ibaraki University. His research interests are in thermophysical properties, structural analysis, noncrystal materials, and nuclear materials.
(tsuyoshi.nishi.75@vc.ibaraki.ac.jp)